https://dx.doi.org/10.1016/j.compgeo.2021.104324

A New Simplified Method for Calculating Short-term and Long-term Consolidation Settlements of Multi-layered Soils Considering Creep Limit

Chen, Ze-Jian (Ph.D. Candidate)
Department of Civil and Environmental Engineering,
The Hong Kong Polytechnic University, Hong Kong SAR, China.
Email: ze-jian.chen@connect.polyu.hk

Feng, Wei-Qiang (Assistant Professor)
Department of Ocean Sciences and Engineering,
The Southern University of Science and Technology, Shenzhen, China.
Email: fengwq@sustech.edu.cn

and
Yin, Jian-Hua (Chair Professor)
Department of Civil and Environmental Engineering,
The Hong Kong Polytechnic University, Hong Kong SAR, China.
Email: jian-hua.yin@polyu.edu.hk

Abstract The long-term consolidation settlement of soft soils under infrastructures is seriously concerned in coastal areas. In practice, soft soil ground is usually composed of multiple layers with different properties, and the effect of soil creep is nonnegligible. However, in conventional consolidation analysis, creep is seldom included during the "primary" consolidation. With conventional creep model, creep strain will reach infinity with time, which is unreasonable in the long-term view. In this study, a new simplified method based on Hypothesis B is presented to calculate both short-term and long-term consolidation settlements of multi-layered soils exhibiting non-linear creep. There are three main characteristics for this new simplified method: (a) the consolidation analysis for multi-layered soil is conducted using spectral method; (b) a nonlinear creep function with creep limit is incorporated to calculate both short-term and long-term creep settlements; (c) the "primary" consolidation and creep are calculated independently and combined with an empirical parameter α together with the consolidation degree U for correcting the creep settlement. Finite element analysis with a self-developed Elastic Visco-Plastic (EVP) constitutive model considering creep limit was also carried out. Verifications by field cases and finite element simulation demonstrate the efficiency and accuracy of the new simplified method in calculating the long-term settlements of soft soil ground under varied engineering conditions. Influences of major parameters selection in the calculation of the new simplified method are also discussed.

Keywords: settlements, nonlinear creep function, multi-layered soft soils, vertical drains, new simplified method

1 Introduction

Constructions of infrastructures and embankments on soft soils have played an important role during the urbanizations around the world in the past decades in many coastal regions, such as Hong Kong, Sweden, Singapore, *etc.* The soft soil ground may be formed by long-term natural sedimentation or reclamation, and consolidation is needed to increase the bearing capacity and stiffness of the soil. Consolidation settlement of soft soil under overlying load is a significant issue, which needs to be predicted accurately and controlled strictly. Conventional simplified calculations are normally based on Terzaghi's 1D consolidation equations, which ignore the inter-layer differences and the creep effect during and after the consolidation. However, natural soft soils usually consist of more than one layers with different values of compressibility, over-consolidation ratio, permeability, *etc.*, which calls for practical analysis method for these complicated situations.

Time-dependent settlements are contributed by the following two process: (1) the increase of effective stress due to dissipation of excess pore water pressure under the applied loading (*i.e*. "primary" consolidation); (2) creep of the soft soil, mainly due to the viscous behaviours of the soil skeleton. Both parts are significant for soft soils and should be considered in the engineering design especially for long-term service. In the earlier years, creep was used to be referred to as "secondary" consolidation, occurring after the end of "primary" consolidation, which is named "Hypothesis A" later. In this hypothesis, the calculations of "primary" consolidation settlements and creep deformation are conducted separately. However, serious concerns have been raised about Hypothesis A, as it fails to satisfy the developing theories in viscous behaviours of clayey soils and usually underestimates the long-term settlements [1–3]. In contrary, Hypothesis B advocates that creep happens during the "primary" consolidation [4], as revealed in Fig. 1. Settlement calculations based on Hypothesis B can be conducted through fully coupled finite element (FE) or finite difference analysis, which may suffer from non-convergence problems. The efficiency and accuracy of fully coupled numerical simulations rely on the proper selection of time steps, numerical algorithm, *etc*. The determination of parameters for 2D and 3D FE analysis is also complicated. Therefore, simplified handy methods for calculating settlements for soft soils based on analytical and empirical calculations are still widely adopted, including the new simplified Hypothesis B methods recently developed for calculating the settlement of single/double layers of soils exhibiting creep [1,5]. Without necessity of iterations on small time-steps, simplified methods consider the total settlements contributed by two parts: the “primary” consolidation settlements and the creep settlements from the time of beginning. A reduction factor on creep settlements was introduced to consider the coupling effect of excess pore pressure dissipation. One of the most important issues in this method is the proper determination of correction factor varied with time and depth. The consolidation analysis for multi-layered soils and modelling of creep behaviors are also necessary.

To predict the time-dependent settlements of soft soils, the first phase of Hypothesis B method is to calculate the degree of consolidation with time under different engineering conditions. Terzaghi’s 1D consolidation equations are developed for a single layer of homogeneous clayey soil under vertical stress. However, Terzaghi’s solutions cannot directly consider horizontal drainage, multi-stage and ramp loading, as well as multi-layered soils with depth-dependent properties. For soft soils with more than one layers, a number of solutions have been developed using different analytical and numerical method for both double-layer [6,7] and general stratified systems [8,9]. These solutions tend to be lengthy and complicated which limits their applications in engineering practice. In another way, Walker et al. [10,11] applied the spectral method to solve consolidation problems for multi-layered soils with high efficiency and accuracy.

The second phase of Hypothesis B method is the calculation of creep deformation with time. The calculation can be accomplished by using an elastic visco-plastic (EVP) constitutive model for clays, which usually considers a correlation between strain and the logarithm of time. Based on 1D straining condition, Bjerrum [12] proposed the "delayed" compression concept, which is later developed into the famous "time line" model. Yin and Graham [13,14] developed this model by introducing the concept of "equivalent time line" and indicated that there exists a unique relationship between the stress-strain state and visco-plastic strain rate. Yin [15] later improved this model with consideration of a creep limit (as shown in Fig. 2) to avoid the logical error in long-term view, and proposed a nonlinear creep function. This model was later developed to a 3D model and implemented in numerical analysis [16–18].

This paper introduces a new Hypothesis B method for calculating the short-term and long-term settlements of multi-layered soft soils under ramp loading. A calculation template embedded with automatically executed VBA program is developed. For the creep strain part, the nonlinear creep function is adopted in the new simplified method. The proposed method was verified by both in-situ measured data and numerical simulations in Plaxis 2D (2015 version). To reveal the influences of permeability and creep parameters selection, sensitivity parametric studies are carried out and discussed.

2 Theoretical frameworks of the new simplified B method for multi-layered soils

2.1 One-dimensional EVP model with creep limit

Fig. 2 shows a schematic diagram for the 1D EVP model [15,17]. For simplicity, the symbols of stresses and strains in Fig. 2 and subsequent figures are in vertical direction by default (*e.g.* $\sigma^{'} = \sigma_z^{'}$) under 1D straining condition. The reference time line (λ-line) and instant time line (κ-line) are determined by conventional laboratory oedometer tests within t_0 period (t_0 could be 24h or the time at end of "primary" consolidation). The visco-plastic strain rate is independent of stress history but uniquely related to the current stress-strain state and can be expressed with equivalent time t_e, which is particular useful in calculating creep settlements for both over-consolidation and normally consolidation soil state. The vertical visco-plastic strain $\Delta\varepsilon^{vp}$ starting from the reference time line is calculated through Eq. (1):

$$\Delta\varepsilon^{vp} = \frac{\frac{\psi_0}{V}\ln\left(\frac{t_0+t_e}{t_0}\right)}{1+\frac{\psi_0}{V\Delta\varepsilon_L}\ln\left(\frac{t_0+t_e}{t_0}\right)} \tag{1}$$

where t_e is the equivalent time, $\frac{\psi_0}{V}$ is the creep coefficient and t_0 is the reference time as the starting point of creep calculation and $\Delta\varepsilon_L$ is the creep strain limit. $\Delta\varepsilon^{vp}$ is equal to $\Delta\varepsilon_L$ when time is infinite. If $\Delta\varepsilon_L$ is taken as infinity, the creep strain calculation is equivalent to the linear logarithmic expression in the EVP model proposed by Yin and Graham [13]:

$$\Delta\varepsilon^{vp} = \frac{\psi_0}{V}\ln\left(\frac{t_0+t_e}{t_0}\right) \tag{2}$$

Fig. 3 shows the schematic diagram of the EVP model for calculating 1D creep settlements. The dashed curves represent the actual stress-strain paths during the consolidation process. $\left(\sigma'_p, \varepsilon_p\right)$ is the pre-consolidation pressure point on the reference time line, which could be calculated with initial OCR if only one single loading step is included. $\left(\sigma'_f, \varepsilon_f\right)$ represents the "final" stress-strain state after consolidation in laboratory under the targeted stress level σ'_f without considering creep. Soil at $\left(\sigma'_f, \varepsilon_f\right)$ could be normally consolidated or over-consolidated, as shown in Figs. 3(a) and 3(b) respectively. t_e can be calculated by Eq. (3):

$$
\begin{aligned}
t_e = t_{e0} + t &= \exp\left[\frac{\Delta\varepsilon_f^{vp}}{\frac{\psi_0}{V}\left(1-\frac{\Delta\varepsilon_f^{vp}}{\Delta\varepsilon_L}\right)}\right] t_0 - t_0 + t \\
&= \exp\left\{\frac{\left[\left(\varepsilon_f-\varepsilon_p\right)-\frac{\lambda}{V}\log\left(\frac{\sigma'_f}{\sigma'_p}\right)\right]}{\frac{\psi_0}{V}\left(1-\frac{\left(\varepsilon_f-\varepsilon_p\right)-\frac{\kappa}{V}\log\left(\frac{\sigma'_f}{\sigma'_p}\right)}{\Delta\varepsilon_L}\right)}\right\} t_0 - t_0 + t, \quad \text{for } \Delta\varepsilon_f^{vp} < \Delta\varepsilon_L
\end{aligned}
\tag{3}
$$

where $\Delta\varepsilon_f^{vp}$ is the difference between the targeted strain ε_f and the reference strain ε_f^r on the reference time line.

Referring to Figs. 2 and 3, we can see that the value of t_e is related to the OCR. For $\left(\sigma'_f, \varepsilon_f\right)$ at normally consolidation state, $\sigma'_f \geq \sigma'_p$ and $\Delta\varepsilon_f^{vp} = 0$, as shown in Fig.3 (a), and therefore $t_e = t$. For $\left(\sigma'_f, \varepsilon_f\right)$ at over-consolidation state, $\Delta\varepsilon_f^{vp}$ is larger than zero, as shown in Fig.3 (b), and $t_e > t$. If $\Delta\varepsilon_f^{vp} \geq \Delta\varepsilon_L^{vp}$, the creep strain rate is zero and there is no creep settlement after loading applied.

2.2 One-dimensional consolidation analysis for multi-layered clayey soils subjected to ramp loading

In Walker's solution[11], the governing equation for consolidation is presented as Eq. (4):

$$\frac{m_v}{\overline{m}_v}\frac{\partial \bar{u}}{\partial t} = -\left[dT_h \frac{\eta}{\overline{\eta}}\bar{u} - dT_v \left(\frac{\partial}{\partial Z}\left(\frac{k_v}{\overline{k}_v} \right)\frac{\partial \bar{u}}{\partial Z} + \frac{k_v}{\overline{k}_v}\frac{\partial^2 \bar{u}}{\partial Z^2} \right) \right] + \frac{m_v}{\overline{m}_v}\frac{\partial \bar{\sigma}}{\partial t} + dT_h \frac{\eta}{\overline{\eta}} w \tag{4}$$

where $\bar{u}$ is the average pore water pressure at certain depth *z*, $\bar{\sigma}$ is the average total stress at certain depth *z*, η is a lumped parameter for consideration of horizontal consolidation, *w* is the water pressure applied on the vertical drains. The volume compressibility m_v is calculated using the total incremental strains resulted from "primary" consolidation. k_v, m_v and η are considered as depth-dependent in a piecewise linear way, which are normalized by a reference layer (with $\overline{k}_v$, $\overline{m}_v$ and $\overline{\eta}$) chosen from all layers. The depth variable $Z = \frac{z}{H}$ is a normalized parameter and H is the total soil thickness. In spectral method, $\bar{u}(Z,t)$ is calculated by integrating over the whole soil depth with a uniform solution expression.

After solving Eq.(4) with spectral method, excess pore water pressure $\bar{u}(Z,t)$ was finally expressed with a series of matrices in Eq.(5):

$$\bar{u}(Z,t) \approx u_0 \mathbf{\Phi v E} (\mathbf{\Gamma v})^{-1} \boldsymbol{\theta} \tag{5}$$

where u_0 is the initial reference excess pore pressure, $\mathbf{\Phi} = \left[\phi_1(Z) \quad \phi_2(Z) \quad \cdots \quad \phi_N(Z) \right]$ is formed by a series of linearly independent sinusoidal basis functions $\phi_j(Z)$, $\mathbf{E}$ is a diagonal matrix associated with the eigenvalues of $\mathbf{\Gamma}^{-1}\mathbf{\Psi} . \mathbf{\Gamma}$, $\mathbf{\Psi}$ and $\boldsymbol{\theta}$ are matrices or vector relevant to soil parameters at any depth and each column of matrix $\mathbf{v}$ is formed by eigenvector associated with each eigenvalue of $\boldsymbol{\Gamma}^{-1}\boldsymbol{\Psi}$. N is the number of terms in $\boldsymbol{\Phi}$, which is normally taken as 30. A larger N produces the more precise results, but requires longer calculation time. Details of the derivation could be found in [10,11].

Walker and Indraratna [19] developed an Excel spreadsheet implemented with VBA program named SPECCON to enable convenience adoption of this method. In the program, consolidation problem of soils with up to 20 layers can be easily calculated. Details of the program can be found in [19].

Geometry parameters of drains, soil layers, vertical and horizontal drainage conditions, permeability, volume compressibility m_v and vertical ramp loading $\Delta\sigma_i'(t)$ are to be input. The output is the average excess pore pressure $\bar{u}_i$ for each layer-i, from which degree of consolidation for layer-i is calculated as $U_i(t) = 1 - \dfrac{\bar{u}_i(t)}{\Delta\sigma_i'(t)}$. Therefore, the "primary" consolidation settlements under loading is obtained by:

$$S_{primary,i}(t) = U_i(t) S_{f,i} \tag{6}$$

where $S_{f,i}$ is the final deformation of layer-i under incremental stress without coupling of excess pore pressure. According to Fig. 3, S_f of a soil element is calculated as:

$$S_f = \begin{cases} H\dfrac{\kappa}{V}\ln\dfrac{\sigma_f'}{\sigma_0'} & \text{(for over-consolidation state)} \\ H\dfrac{\kappa}{V}\ln\dfrac{\sigma_p'}{\sigma_0'} + H\dfrac{\lambda}{V}\ln\dfrac{\sigma_f'}{\sigma_p'} & \text{(for normal-consolidation state)} \end{cases} \tag{7}$$

where H is the thickness of the element. It should be noted that for soils under ramp loading $\Delta\sigma'(t)$, both $\sigma_f'(t)$ and $S_f(t)$ are time-dependent within the construction time.

Considering the nonlinearity of soil behavior, compression strain under a stress increment varies with different depths due to different initial effective stress. Therefore, $S_{f,i}$ for each layer should be calculated by precise integration over the layer thickness H_i or by approximation as the sum of S_f in many smaller sub-layers.

In this study, each soil layer is divided into sub-layers with thickness of 0.5m at most, if $H_i \geq 0.5\text{m}$. For each sub-layer, the difference of initial effective stress between the upper and lower boundary is around 2.5 kPa for a clay with density of 15 kPa/m, which should be small enough since the in-situ vertical stress will be much larger for thick layers of soils. The thickness of 0.5m for sub-layers have also been adopted and examined in [1,5,20]. Thus $S_{f,i}$ is calculated as:

$$S_{f,i} = \sum_{k=1}^{\Pi\left(\frac{H_i}{0.5\text{m}}\right)} S_{fi,k} \tag{8}$$

where *k* denotes the number of sub-layer. With $S_{f,i}$, $m_{v,i}$ is computed as $m_{v,i} = \frac{S_{f,i}}{H_i \Delta\sigma'}$ before consolidation analysis.

2.3 Calculation of total time dependent settlements with Hypothesis B

According to Hypothesis B, creep starts before end of "primary" consolidation, which results the complexity of stress-strain state determination. The total settlements for each layer include two parts: the settlement resulted from excess pore pressure dissipation and the other from creep deformation, as shown in Eq. (9):

$$S(t) = S_{primary}(t) + S_{creep}(t) \tag{9}$$

where $S_{primary}(t)$ is the incremental settlements caused by "primary" consolidation, as calculated by Eq. (6) in the last section. S_{creep} is the settlements caused by soft soil creep. The calculation of $S_{creep}(t)$ is shown in Eq. (10):

$$S_{creep}(t)=\begin{cases}\alpha U S_{creepf}(t) & t\le t_{EOP}\\ \alpha U S_{creepf}(t)+(1-\alpha U)S_{creepd}(t) & t>t_{EOP}\end{cases} \tag{10}$$

In Eq. (10), S_{creep} after EOP (when the degree of "primary" consolidation reaches 98%) contains two terms: S_{creepf} and S_{creepd}. S_{creepf} corresponds to the assumption that creep occurs immediately after application of loading within reference time t_0, without considering excess pore pressure dissipation. S_{creepd} corresponds to Hypothesis A that creep only occurs after EOP. As the effective stress increment is delayed by excess pore pressure dissipation, S_{creepf} will apparently overestimate the actual creep settlements before EOP. Therefore, S_{creepf} is multiplied with an empirical correction coefficient α and average consolidation degree *U*, both ranging between 0 and 1. When $\alpha=1$, Eq. (10) become equivalent to Hypothesis A method. In some previous studies [5,21], $\alpha=0.8$ was frequently adopted and validated for different clayey soils under different conditions. However, *U* was not included yet, resulting in overestimation at the earlier stages for the thick soil layers.

According to the one-dimensional EVP model, the calculation formula for S_{creepf} and S_{creepd} is shown in Eqs. (11) and (12):

$$S_{creepf}(t)=H\left[\frac{\frac{\psi_0}{V}\ln\left(\frac{t_0+t_e}{t_0}\right)}{1+\frac{\psi_0}{V\Delta\varepsilon_L}\ln\left(\frac{t_0+t_e}{t_0}\right)}-\Delta\varepsilon_f^{vp}\right]\quad (\text{for } t\ge t_0) \tag{11}$$

$$S_{creepd}\left(t\right)=H\left[\frac{\frac{\psi_0}{V}\ln\left(\frac{t_0+t_e}{t_{EOP}}\right)}{1+\frac{\psi_0}{V\Delta\varepsilon_L}\ln\left(\frac{t_0+t_e}{t_{EOP}}\right)}-\Delta\varepsilon_f^{vp}\right] \quad (\text{for } t\geq t_{EOP}) \tag{12}$$

where t_{EOP} is the elapsed time at end of "primary" consolidation. Other symbols have been explained in previous paragraphs. It should be noted that for soils under ramp loading $\Delta\sigma^{'}\left(t\right)$, $\Delta\varepsilon_f^{vp}\left(t\right)$ could be time-dependent during the construction time.

The average consolidation degree for each layer is $U_i\left(t\right)=1-\frac{\bar{u}_i\left(t\right)}{\Delta\sigma_i'\left(t\right)}$. If there are more than one loading stages, αU_i for creep calculation in Eq. (10) should be replaced by $\alpha U_{multi,i,j}$ in for layer-*i* at stage-*j* with the following equation:

$$U_{multi,i,j}\left(t\right)=1-\frac{\sum_{k=1}^{j}\bar{u}_{i,k}\left(t\right)}{\sigma_{i,j}\left(t\right)-\sigma_{i0}} \tag{13}$$

where $\bar{u}_{i,k}\left(t\right)$ is the average excess pore water pressure of layer-*i* at stage-*j*, $\sigma_{i,j}\left(t\right)$ is the loading stage after the *j*-th loading and σ_{i0} is the initial value of *j*-th loading.

The calculation process of the proposed simplified method has been developed into automatically executed Excel spreadsheets using VBA programming language, in which stratified soil ground with maximum of 20 layers under ramp loading can be directly modeled and analyzed. The flow chart of the program is presented in Fig. 4.

3 Programming of EVP model for fully coupled finite element analysis

Based on Yin (1999)'s theory, a 3D EVP models [16,17] were developed based on the overstress theory [22,23]. The model had been validated by numbers of element tests in previous studies, while simulations on large-scale field cases are still lacking. In this study, a 3D EVP constitutive model based on the abovementioned model was encoded in the user-defined modulus of Plaxis 2015 to enable finite element analysis as comparisons.

3.1 Framework of the 3D EVP model

In 3D stress-strain space, the strain rate of soil is divided into elastic and visco-plastic parts, as shown in Eqs. (14a-14c):

$$\dot{\varepsilon}_{ij} = \dot{\varepsilon}_{ij}^{vp} + \dot{\varepsilon}_{ij}^{e} \tag{14a}$$

$$\dot{\varepsilon}_{ij}^{e} = C_{ijkl}\dot{\sigma}_{ij}^{'e} \qquad k = 1,2,3 \text{ and } l = 1,2,3 \tag{14b}$$

$$\dot{\varepsilon}_{ij}^{vp} = \gamma\langle\phi(F)\rangle\frac{\partial f}{\partial\sigma_{ij}^{'}} = S\frac{\partial f}{\partial\sigma_{ij}^{'}} \tag{14c}$$

where subscript i and j represent the generalized stress-strain condition, $\dot{\varepsilon}_{ij}^{e}$ is the elastic strain rate, $\dot{\varepsilon}_{ij}^{vp}$ is the visco-plastic strain rate, C_{ijkl} is the elastic compliance tensor, f is the load potential function and $f = 0$ is the yielding surface in Cam-Clay model. $\gamma\langle\phi(F)\rangle$ is a function dependent on the position of the yielding surface, in which F describes the difference between the current yielding surface and a reference yielding surface. $\gamma\langle\phi(F)\rangle$ can be replaced by a scaling function S, as proposed in [16]. Eq. (14a) can thus be transferred to Eq. (15):

$$\dot{\varepsilon}_{ij} = \left(\frac{1}{2G^{e}}\dot{s}_{ij} + \frac{p^{'}}{3K^{e}}\dot{\delta}_{ij}\right) + S\frac{\partial f}{\partial\sigma_{ij}^{'}} \tag{15}$$

where $K^e = \frac{Vp^{'}}{\kappa}$ is the bulk modulus and $G^e = \frac{2(1-2\nu)K^e}{2(1+\nu)}$ is the shear modulus, $V = 1 + e_0$ is the initial specific volume, $p^{'} = \frac{tr(\sigma_{ij}^{'})}{3} = \frac{\sigma_{11}^{'} + \sigma_{22}^{'} + \sigma_{33}^{'}}{3}$ is the mean effective stress, $s_{ij} = \sigma_{ij}^{'} - \delta_{ij} p^{'}$ is the deviatoric stress tensor, and $\delta_{ij} = \begin{cases} 1 & i = j \\ 0 & i \neq j \end{cases}$ is a Kronecker delta.

The flow direction of the visco-plastic strain is controlled by the load potential function in Eq. (16):

$$f = \frac{q^2}{M^2 p^{'}} + p^{'} - p_m^{'} = \frac{3s_{ij} : s_{ij}}{2M^2 p^{'}} + p^{'} - p_m^{'} \tag{16}$$

where *M* is the slope of critical state line in $p^{'} - q$ space and $p_m^{'}$ describes the position and size of current yielding surface, as shown in Fig. 5.

According to Eq. (14c), determination of the value of *S* is important for calculation of visco-plastic strain rate in each time step. Based on Eq. (14c), it can be derived that:

$$S = \frac{\dot{\varepsilon}_v^{vp}}{\left|\frac{\partial f}{\partial p'}\right|} \tag{17}$$

where $\dot{\varepsilon}_v^{vp}$ is the visco-plastic volumetric strain rate. In Fig. 5, the visco-plastic volumetric strain rate on the same yielding surface is the same, and therefore $\dot{\varepsilon}_v^{vp}$ at point $(p^{'}, q)$ is the same as $\dot{\varepsilon}_{vm}^{vp}$, resulting in Eq. (18):

$$\dot{\varepsilon}_v^{vp} = \dot{\varepsilon}_{vm}^{vp} = \frac{\psi_0}{Vt_0}\left(1+\frac{\left(\varepsilon_{vm}^r-\varepsilon_{vm}\right)}{\Delta\varepsilon_L}\right)^2 \exp\left\{\frac{V\left(\varepsilon_{vm}^r-\varepsilon_{vm}\right)}{\psi_0\left[1+\frac{\left(\varepsilon_{vm}^r-\varepsilon_{vm}\right)}{\Delta\varepsilon_L}\right]}\right\} \tag{18}$$

where ε_{vm} and ε_{vm}^r locate at the current equivalent time line and referent time line respectively in the $\varepsilon_{vm} - \ln p_m^{'}$ space, which can be calculated by Eqs. (19a) and (19b):

$$\varepsilon_{vm} = \varepsilon_v + \frac{\kappa}{V}\ln\frac{p_m^{'}}{p^{'}} \tag{19a}$$

$$\varepsilon_{vm}^r = \varepsilon_{vm0}^r + \frac{\lambda}{V}\ln\frac{p_m^{'}}{p_{mr0}^{'}} \tag{19b}$$

where $p_{vmr0}^{'}$ and ε_{vm0}^r are fixed points on the reference time line.

3.2 Algorithm in the finite element analysis

The constitutive model was programed with Fortran language using the “user-defined soil model” module in Plaxis (2015 version). In a calculation step, the software passes the computed stresses, strains and other state parameters to the kernel with constitutive model. The new stress-strain state will be returned by the constitutive model after iterations.

In the initial state, the value of $p_{m0}^{'}$ is calculated using POP (pre-over consolidation pressure, $POP = \sigma_{zp}^{'} - \sigma_{z0}^{'}$) or OCR with modification from K_0-consolidation to isotropic consolidation, as shown in Fig.5. During the consolidation analysis, with the strain and time increment produced through global iterations in the software, the visco-plastic strain increment (in vector form) was calculated with Euler time integration scheme [24] as shown in Eq.(20):

$$\Delta\boldsymbol{\varepsilon}^{vp,n} = \Delta t\cdot\left[\left(1-\theta\right)\cdot\Delta\dot{\boldsymbol{\varepsilon}}^{vp,n} + \theta\cdot\Delta\dot{\boldsymbol{\varepsilon}}^{vp,n+1}\right] \tag{20}$$

in which Δt is the time increment from n to n+1 stage, $\theta \in [0,1]$ is used to adjust the Euler integration scheme from fully explicit to fully implicit integral. In this study, θ was set as 0.5, which involves the advantages of both explicit and implicit methods with fairly efficiency and sufficient accuracy in FE analysis [25]. The increment of effective stress is determined by:

$$\Delta\boldsymbol{\sigma} = \mathbf{D} : \Delta\boldsymbol{\varepsilon}^{e} = \mathbf{D} : \left(\Delta\boldsymbol{\varepsilon} - \Delta\boldsymbol{\varepsilon}^{vp}\right) \tag{21}$$

where **D** is the elastic stiffness vector. To solve Eqs. (20)-(21), the Newton-Raphson iteration scheme is conducted with Taylor series, as shown in Eq. (22):

$$\begin{cases} \boldsymbol{\sigma}^{n+1} = \boldsymbol{\sigma}^{i} + d\boldsymbol{\sigma}^{i} \\ \dot{\boldsymbol{\varepsilon}}^{vp,n+1} = \dot{\boldsymbol{\varepsilon}}^{vp,i} + \dfrac{\partial \dot{\boldsymbol{\varepsilon}}^{vp,i}}{\partial \boldsymbol{\sigma}} d\boldsymbol{\sigma} \end{cases} \tag{22}$$

where $\boldsymbol{\sigma}^{i}$ is the new stress vector and the iteration is finished once the value of $\left|d\boldsymbol{\sigma}^{i}\right|$ is small enough.

4 Verification of the new simplified Hypothesis B method with in-situ measured data and finite element simulations

Computations on one field case were conducted using the proposed new simplified method. The test field is an embankment on a natural soft soil ground in Sweden without vertical drains and has been monitored for more than 50 years from 1947. The calculation results from the proposed new simplified method are presented in this section and compared with measured data. Numerical simulations using FE program Plaxis are also presented and compared.

4.1 Description of the Väsby embankment

In 1945, in order to select a suitable construction site for the new airfield, a field test was conducted by Swedish Geotechnical Institute (SGI) at the farm of Lilla Mellösa near Upplands

Väsby, Sweden. The field ground contains thick layers of soft soils, with high water content and volume compressibility. Three test fills with and without vertical drains were constructed from 1945 to 1947, for which monitoring works on the settlements and pore pressure were continued to recent years. Continuous settlements during the 60 years have been noticed and discussed by a number of researchers [26,27], especially the "undrained" fill (*i.e.*, the one without installation of vertical drains). The settlements are probably due to slow "primary" consolidation and long-term creep deformation. In this study, the new simplified method is used to calculate the settlements for one of the "undrained" fills. The profiles section of the test embankment is shown in Fig. 6. According to the results of ground investigation [28][26], the ground in Väsby consists of at least four types of soft clay, but without distinct boundaries. Under the soft clay there exist a thin layer of medium grey sand and therefore the field was considered as a two-way drainage system in the calculations. Due to the large dimensions of embankment, the total vertical settlement at the center of the embankment could be considered as a one-dimensional problem.

Construction was started in Nov. 1947, with a 2.5m-high fill of gravels with unit weight of around 16.2 kN/m^3, constituting a vertical loading of around 40.6 kPa and was finished in 25 days. The loading could be considered as a ramp-increased total vertical stress uniformly distributed on the top surface of the soil. In-situ measuring on both the pore pressure and the settlements was started from the year of construction and has continued to recent years. A series of settlement markers and piezometers were placed in different layers to monitor the settlements and pore pressure.

4.2 Soil parameters and numerical model

Borehole samples at different depths were taken from the site and tested in laboratories to provide the permeability parameters, water content, compression curves, etc. In this study, the whole soils with thickness of 14 m in total are divided into 15 different layers. During calculations of S_f and m_v, each layer is divided into more than one sub-layers as mentioned in 2.2. Most of the parameters for each layer, including the compression indices and permeability, were obtained according to the published report by Chang [28] and Larsson and Mattson [26], as listed in Table 2. κ and λ were fitted using the data at the time of end of "primary" consolidation (EOP). For creep behaviours, there are three major parameters: creep coefficient ψ_0, creep strain limit $\Delta\varepsilon_L$ and reference time t_0, which are not available for each layer in the original reports. In this study, the parameters were fitted with the original data from an oedometer test in [28] using the method by Yin [15]. The loading step for the sample was from 40 to 80 kPa, and the strain-time curve in 24 hours was provided in [28], as shown in Fig. 7(a). Since the vertical surcharge was 40.6 kPa in the field while the initial vertical stress was from 0 to around 80 kPa along the soil depth, it is reasonable to use the data from this test to estimate the creep parameters. With these data, ψ_0 and $\Delta\varepsilon_L$ can be fitted using Eq. (23) transferred from Eq. (4):

$$\ln\left(\frac{t_0+t_e}{t_0}\right)/\Delta\varepsilon^{vp} = \frac{V}{\psi_0} + \frac{1}{\Delta\varepsilon_L}\ln\left(\frac{t_0+t_e}{t_0}\right) \tag{23}$$

where t_0 was chosen as t_{EOP} in the oedometer test, which was 130 min. As the sample was normally consolidated under 40 to 80 kPa, t_0+t_e equal to t_0+t, where t is the elapsed time in the test. After plotting $\ln\left(\frac{t_0+t}{t_0}\right)/\Delta\varepsilon^{vp}$ versus $\ln\left(\frac{t_0+t}{t_0}\right)$ in Fig. 7(b), $\frac{V}{\psi_0}$ is the intercept and $\frac{1}{\Delta\varepsilon_L}$ is the slope, so $\frac{\psi_0}{V}$ and $\Delta\varepsilon_L$ can be determined as 0.014 and 0.22 respectively. The fitted strain-ln(time) curve by the EVP model is shown in Fig. 7(c), which is highly identical to the test data. Therefore, $\psi_0 = \frac{\psi_0}{V}(1+e_0) = 0.014 \times 4.15 = 0.058$ and $\Delta e_L = \Delta \varepsilon_L \left(1+e_0\right) = 0.22 \times 4.15 = 0.898$ could be obtained. Δe_L is the limit of change in void ratio under creep condition. For different soil layers, both ψ_0 and Δe_L were assumed the same for simplicity.

In this paper, both the new simplified B method and FE simulation in Plaxis is conducted and compared with measured data. The FE simulation was conducted in Plaxis with the nonlinear EVP model in Section 3. The soil ground was built up as a plane strain model, however, with assumption that the center of the embankment deformed under 1D straining condition. The width of the soil ground was selected to be 1m. The numerical model after meshing is shown in Fig. 8.

4.3 Comparisons of calculation results by simplified B method with FE simulation and measured data

In the new simplified B method, $\alpha = 0.8$ was used as the correction parameter. Since $\alpha = 0.8$ has been adopted and examined in many studies, it would be meaningful to adopt the same value for the new method and new case in this study. The calculation results are presented in Figs. 9(a)-(d). According to the figures, the computed settlement curves at different depths by the new simplified B method were highly reliable during the whole process compared with the results by FE simulation and in-situ measured data, only with minor differences. At the earlier stages, , the settlements at the lower positions by new simplified B method were a bit larger than the measured data. The less precise results for the beginning period might be due to the delayed consolidation by visco-plastic strain, which cannot be considered in the new simplified method, as it is not fully coupled analysis. At the final stages, the three sets of curves become highly consistent.

The comparisons of excess pore pressure distribution are presented in Fig. 10. For the earlier stages, FE simulation gives relatively more accurate pore pressure distribution with measured ones. However, the measured excess pore pressure tends to be lower than those calculated in 1968 and 1979 while higher in the latest stage in 2002, possibly due to the changes of permeability with time. It is also revealed that the new simplified method generally underestimates the excess pore pressure even in the earlier stages, which is related to the lack of fully coupled analysis for consolidation and creep. From the results of the two cases, it is indicated that compared to settlement prediction, the new simplified method is less reliable in prediction of excess pore pressure dissipation.

The settlement components $S_{primary,i}$ and $S_{creep,i}$ (consisting of $S_{creepf,i}$ and $S_{creepd,i}$) at different depths by the simplified B method were plotted against time in Fig.11 and Fig.12. Compared with $S_{primary,i}$, the distribution of $S_{creep,i}$ was more uniform with soil depth. Although the primary compression of soil layers below 7.5m only contributed 1/3 among all soil layers, their creep settlement contributed more than 50%, since their POPs and creep parameters were similar to the higher layers. Fig.13 shows the evolution of $S_{primary}$, S_{creepf} and S_{creepd} for the whole soil layers with time, which indicates that creep played an important role in the total settlement of the embankment. S_{creepd} was much smaller than S_{creepf} and occurred at a very late stage, since the “primary” consolidation process for most of the layers cost a long period.

5 Parameter sensitivity analysis of the new simplified B method

In the past section, the new simplified method performs well in settlements predictions for the real embankment. It should be noted that the analysis results can be influenced by selection of parameters, especially the correction parameter α and soil properties. In this study, the effect of these parameters will be investigated, and the their selection principles and techniques will be discussed.

5.1 The effect of correction parameter α

Fig. 14 compares the total settlement curves from the new simplified method using different values of α, with FE simulation as well as measured data. According to Fig. 14, the choice of α has significant influence on the prediction. The use of $\alpha = 0$, which is corresponding to Hypothesis A, results in severe underestimation on the settlements during the whole process. Using $\alpha = 0.6$ also underestimate the settlements while using $\alpha = 1$ overestimates the settlements. If a single parameter $\alpha = 0.8$ is used without multiplying *U* in Eq. (10), which is the original method by Yin and Feng [5], the settlement curve is also inaccurate before the final state. These results again demonstrate the necessity of adopting suitable value of α before *U*. For this case, it is shown that $\alpha = 0.8$ is the optimal value, which has also been examined for different cases in previous studies [1,5].

5.2 The effect of creep parameters $\Delta\varepsilon_L$ *and* ψ_0

According to Yin (1999)'s model, the nonlinear creep parameters $\Delta\varepsilon_L$ and ψ_0 are inter-dependent and could be fitted simultaneously, as shown in Section 4. However, very few existing projects paid attention to this effect and the corresponding parameters are frequently difficult to determine due to lack of long-term oedometer test data. To demonstrate the influence of creep parameters on settlement calculations, different values of $\Delta\varepsilon_L$ and ψ_0 will be used in the calculations for comparisons.

The values of $\Delta\varepsilon_L$ and ψ_0 were adjusted based on the oedometer test data in the previous section. From an aspect of physics, the value of $\Delta\varepsilon_L$ might range within $\left(0, \frac{e}{1+e_0}\right]$, where *e* is the void ratio at the reference time line under a certain stress state. By adopting different values of $\Delta\varepsilon_L$ and ψ_0 can be fitted with test data through the following equation:

$$\frac{\Delta\varepsilon^{vp}V}{\left(1-\frac{\Delta\varepsilon^{vp}}{\Delta\varepsilon_L}\right)}=\psi_0\ln\left(\frac{t_0+t_e}{t_0}\right) \tag{24}$$

By plotting the left side in Eq. (24) against $\ln\left(\frac{t_e+t_0}{t_0}\right)$, ψ_0 was fitted as the slope of the curve. Eq.(24) could also be used for fitting conventional creep coefficient ψ in Yin and Graham's EVP model [29], with $\Delta\varepsilon_L=+\infty$.

A total of four sets of $\Delta\varepsilon_L$, Δe_L and ψ_0 for the oedometer sample were obtained through in this method, as listed in Table 2. In settlement calculations, Δe_L and ψ_0 were assumed the same for all layers. For case III, $\Delta\varepsilon_L=10000$ was adopted for the new simplified method and the nonlinear EVP model in Plaxis.

Figs. 15(a) to (c) show the calculation results with different creep parameters by both the new simplified B method and FE analysis. It is indicated that although the parameters were fitted with the same set of laboratory test data, the settlements came out to be highly different in the field scale. In Fig. 15(a), the calculation by both the new simplified method and FE analysis using $\Delta\varepsilon_L=0.1$ caused significant underestimation on the total settlement, especially in the long-term view. In Fig. 15(b) with $\Delta\varepsilon_L=\frac{e}{1+e_0}$, the calculated settlement curves were larger than the measured ones. In Fig. 15(c), using $\Delta\varepsilon_L=+\infty$ caused the highest overestimation.

The Soft Soil Creep (SSC) model in Plaxis [30] was also used in the calculation of Case III, in which no creep limit was considered. It can be found that FE analysis results by the self-developed EVP model were larger than the results by SSC model. The main reason is the different values of t_0, which is 130 min in EVP model and 1 day in SSC. A larger t_0 will result in smaller value of $\ln\left(\frac{t_e + t_0}{t_0}\right)$ with elapsed time and reduce the creep strain. After changing t_0 into 1 day manually, the simulated curves by EVP model was highly close to the one by SSC model. Therefore, t_0 has a significant influence on the calculations. The use of t_0 should be kept in consistency with the position of reference time line, the compression parameters for "primary" consolidation and creep parameters, as revealed in Fig. 2.

Therefore, accurate determination of ψ_0, $\Delta\varepsilon_L$ and t_0 according to laboratory tests is highly recommended for engineering constructions especially for the long-term design.

5.3 The effect of permeability k_v

In consolidation analysis, permeability values of k_v vary with void ratio of soft clays. For engineering design, it is convenient to adopt constant reasonable permeability parameters during the consolidation process, and the selection of k_v therefore becomes an important technical issue. As indicated the last section, averaged values of k_v before and after the loading is appropriate for predictions in both cases. In this sub-section, settlement calculations with different permeability parameters before and after loading were conducted. The permeability before and after loading in Väsby Embankment were provided by Larsson and Mattsson [26] through laboratory tests, as listed in Table 3.

Figs. 16(a) to (b) show the results of settlement predictions with different values of permeability. For both cases, the results by the new simplified method and FE analysis were still fairly close. In addition, the choice of permeability parameters has significant effect on the prediction curves for both cases. Using initial permeability value, the settlements tend to develop faster at the earlier stage but get close to the measured results at the end of consolidation. Comparatively, the settlements develop very slowly when using the final permeability value, which will cause underestimation for most of the time.

Therefore, average permeability parameters are recommended for settlement analysis. For other cases where permeability after the consolidation is unavailable, empirical correlations might be used to calculated the change of k_v with estimated void ratio [31].

5.4 Verifications of the new simplified method for embankments subjected to more than one loading stages

In Väsby Embankment, only one loading stage is involved. As presented in Fig. 4, the proposed simplified method can be applied in multi-staged loading conditions. In this study, additional loading stages will be added in the case. In Stage 1, vertical stress of 40.6 kPa was applied in 25 days. After 100 days of consolidation, the vertical load was increased to 100 kPa in 25 days in Stage 2, lasting for 20000 days. In Stage 3, the vertical load was reduced to 40.6 kPa in 25 days and kept for 20000 days.

Both FE analysis and simplified Hypothesis B method are used for the calculation. The looping method in flow chart of Fig. 4 was used to calculate the consolidation settlements at three stages. Despite the absence of measured data, the fully coupled FE analysis can be used as verification for the proposed simple method. The calculated settlements at different depths are shown in Figs 17 (a)-(d). According to these figures, the settlement curves by simplified Hypothesis B method are highly close to those by FE simulations under three stages of loading and unloading.

5 Conclusions

This paper proposed a new simplified method based on Hypothesis B to calculate time-dependent settlements for multi-layered soft soils with a nonlinear creep function considering creep limit. This method can be conveniently operated using Excel spreadsheet with high efficiency and stability. Walker's solution with spectral method is adopted in the "primary" consolidation analysis for the multi-layered system. Yin's nonlinear creep function with a creep limit is used for creep analysis. The consolidation and creep settlements are combined by involving a correction factor αU in the formulation. FE analysis was also carried out in Plaxis with a self-encoded 3D EVP model based on Yin's nonlinear creep function. The calculation results of the new simplified method are verified using in-situ measured data and compared with FE simulations for a real case in Sweden. Contributions of different components of settlements subjected to primary consolidation and creep are clearly demonstrated by the proposed method. A series of parametric studies have been carried out to investigate the effect of parameters determination on the settlement calculations. Several important conclusions can be drawn from this study:

1) The proposed simplified B method is able to predict the settlements with high accuracy. Compared with FE simulations, the new simplified B method can be used to calculate similar results with much higher stability and efficiency without any convergence difficulties.
2) The excess pore pressure calculated in the new simplified method was lower compared with in-situ measurement and numerical simulations, which is reasonable since the consolidation analysis and creep analysis were decoupled.
3) Compared with other values, the use of $\alpha = 0.8$ in the new simplified B method is the optimal.

4) Different adoptions of creep parameters ψ_0 and $\Delta\varepsilon_L$ will result in different results in the calculations, especially for the long-term prediction. It is highly recommended for engineering designers to use proper values of ψ_0 and $\Delta\varepsilon_L$ according to the long-term laboratory oedometer tests.
5) The selection of permeability has significant influences on the settlement calculations. The use of averaged permeability before and after loading tests performs well in the predictions.
6) With comparisons to FE simulations, the proposed method performs well in settlement calculations for multi-layered soils under multi-staged loading and unloading conditions.

Due to considerations of convenience in practice, complicated soil conditions such as lateral drainage, horizontal deformation, soil anisotropy and spatial variations of soil properties were yet not included in the proposed method. Further improvements based on these issues are worth of study to widen the range of applications of the simplified Hypothesis B method without much hurting of the convenience.

Acknowledgements

The work in this paper is supported by a Research Impact Fund (RIF) project (R5037-18), and three General Research Fund (GRF) projects (PolyU 152209/17E; PolyU 152179/18E; PolyU 152130/19E) from Research Grants Committee (RGC) of Hong Kong Special Administrative Region Government of China. The authors also acknowledge supports from Research Institute for Sustainable Urban Development, Research Centre for Urban Hazards Mitigation, and three grants (BBAG, ZDBS, ZVNC) of The Hong Kong Polytechnic University.

References

[1] Feng WQ, Yin JH. A new simplified Hypothesis B method for calculating consolidation settlements of double soil layers exhibiting creep. Int J Numer Anal Methods Geomech 2017;41:899–917. https://doi.org/10.1002/nag.2635.

[2] Le TM, Fatahi B, Khabbaz H. Viscous Behaviour of Soft Clay and Inducing Factors. Geotech Geol Eng 2012;30:1069–83. https://doi.org/10.1007/s10706-012-9535-0.

[3] Kabbaj M, Tavenas F, Leroueil S. In situ and laboratory stress-strain relationships. Géotechnique 1988;38:83–100. https://doi.org/10.1680/geot.1988.38.1.83.

[4] Ladd C, Foott R, Ishihara K, Schlosser F, Poulos H. Stress-Deformation and Strength Characteristics. State Art Report, Proceeding 9th ISMFE, vol. 2, Tokyo: 1977, p. 421–494.

[5] Yin J-H, Feng W-Q. A new simplified method and its verification for calculation of consolidation settlement of a clayey soil with creep. Can Geotech J 2017;54:333–47. https://doi.org/10.1139/cgj-2015-0290.

[6] Xie K, Xie X, Jiang W. Study on Non Linear Consolidation Theory on Double Layered Soils. Comput Geotech 2002;29:151–68.

[7] Zhu G, Yin J-H. Solution charts for the consolidation of double soil layers. Can Geotech J 2005;42:949–56. https://doi.org/10.1139/t05-001.

[8] Nogami T, Li M. Consolidation of clay with a system of vertical and horizontal drains. J Geotech Geoenvironmental Eng 2003. https://doi.org/10.1061/(ASCE)1090-0241(2003)129:9(838).

[9] Chen RP, Zhou WH, Wang HZ, Chen YM. One-dimensional nonlinear consolidation of multi-layered soil by differential quadrature method. Comput Geotech 2005;32:358–69. https://doi.org/10.1016/j.compgeo.2005.05.003.

[10] Walker R, Indraratna B. Consolidation analysis of a stratified soil with vertical and horizontal drainage using the spectral method. Géotechnique 2009;59:439–49. https://doi.org/10.1680/geot.2007.00019.

[11] Walker R, Indraratna B, Sivakugan N. Vertical and Radial Consolidation Analysis of Multilayered Soil Using the Spectral Method. J Geotech Geoenvironmental Eng 2009;135:657–63. https://doi.org/10.1061/(asce)gt.1943-5606.0000075.

[12] Bjerrum L. Engineering geology of Norwegian normally-consolidated marine clays as related to settlements of buildings. Géotechnique 1967:81–118. https://doi.org/10.1680/geot.1967.17.2.83.

[13] Yin JH, Graham J. Viscous-elastic-plastic modelling of one-dimensional time-dependent behaviour of clays. Can Geotech J 1989. https://doi.org/10.1139/t89-029.

[14] Yin J-H, Graham J. Equivalent times and one-dimensional elastic viscoplastic modelling of time-dependent stress-strain behaviour of clays. Can Geotech J 1994. https://doi.org/10.1139/t94-005.

[15] Yin J-H. Non-linear creep of soils in oedometer tests. Géotechnique 1999;49:699–707. https://doi.org/10.1680/geot.1999.49.5.699.

[16] Yin J-H, Graham J. Elastic viscoplastic modelling of the time-dependent stress–strain behaviour of soils. Can Geotech J 1999:736–45.

[17] Yin JH, Zhu JG, Graham J. A new elastic viscoplastic model for time-dependent behaviour of normally and overconsolidated clays: Theory and verification. Can Geotech J

2002;39:157–73. https://doi.org/10.1139/t01-074.
[18] Feng W. Experimental Study and Constitutive Modeling of the Time-dependent Stress-Strain Behavior of Soils. 2016.
[19] Walker R, Indraratna B. A Microsoft Excel spreadsheet program for vertical and radial consolidation analysis of multi layered soil using the spectral method. <http:// www.uow.edu.au/eng/research/geotechnical/software/index.html> 2008.
[20] Yin J-H, Zhu G. Consolidation Analyses of Soils. 1st ed. CRC Press; 2020.
[21] Feng WQ, Lalit B, Yin ZY, Yin JH. Long-term Non-linear creep and swelling behavior of Hong Kong marine deposits in oedometer condition. Comput Geotech 2017;84:1–15. https://doi.org/10.1016/j.compgeo.2016.11.009.
[22] Perzyna P. Fundamental Problems in Viscoplasticity. Adv Appl Mech 1966. https://doi.org/10.1016/S0065-2156(08)70009-7.
[23] Perzyna P. The constitutive equations for rate sensitive plastic materials. Q Appl Math 1963;20:321–32. https://doi.org/10.1090/qam/144536.
[24] Katona MG. Evaluation of viscoplastic cap model. J Geotech Eng 1984. https://doi.org/10.1061/(ASCE)0733-9410(1984)110:8(1106).
[25] Yin Z-Y, Li J, Jin Y-F, Liu F-Y. Estimation of Robustness of Time Integration Algorithms for Elasto-Viscoplastic Modeling of Soils. Int J Geomech 2019;19:04018197. https://doi.org/10.1061/(asce)gm.1943-5622.0001351.
[26] Larsson R, Mattsson H. Settlements and shear strength increase below embankments 2003:1–98. https://doi.org/10.1021/JM100506Y.
[27] Le TM. Analysing Consolidation Data to Optimise Elastic Visco – plastic Model Parameters for Soft Clay. University of Technology, Sydney (UTS), 2015.
[28] Chang YCE. Long term consolidation beneath the test fills at Väsby. 1981.
[29] Yin J-H, Graham J. Visco-elastic-plastic modelling of one-dimentional time-dependent behaviour of clays. Can Geotech J 1989;26:199–208.
[30] Vermeer PA, Neher HP. A soft soil model that accounts for creep. Beyond 2000 Comput Geotech 2019:249–61. https://doi.org/10.1201/9781315138206-24.
[31] Tavenas F, Jean P, Leblond P, Leroueil S. The permeability of natural soft clays. Part II: permeability characteristics. Can Geotech J 1983;20:645–60. https://doi.org/10.1139/t83-073.

Captions of Figures

Fig. 1 The schematic diagram of the difference between Hypothesis A and Hypothesis B

Fig. 2 The schematic diagram of the 1-D nonlinear EVP model

Fig. 3 The schematic diagram of creep calculation when the final stress-strain of soil $\left(\sigma_f^{'}, \varepsilon_f\right)$ is at: (a) normally consolidation state and (b) over-consolidation state

Fig. 4 The calculation flow chart of the new simplified Hypothesis B method

Fig. 5 The schematic diagram of the 3-D nonlinear EVP model

Fig. 6 The ground profile of the Väsby embankment

Fig. 7 Fitting of creep parameters with the oedometer test results: (a) the original strain-log(time) curve; (b) plotting of $\ln\left(\frac{t_0+t}{t_0}\right)/\Delta\varepsilon^{vp}$ v.s. $\ln\left(\frac{t_0+t}{t_0}\right)$; (c) comparison of fitting results and test data

Fig. 8 Numerical model in Plaxis with mesh

Fig. 9 Comparisons of settlement curves by simplified Hypothesis B method, FE simulations and measurement at different depths: (a) 0m; (b) 2.5m; (3) 5m and (4) 7.5m

Fig. 10 Comparisons of excess pore pressure distributions in Year 1968, 1979 and 2002 by the new simplified Hypothesis B method, FE simulation and in-situ measurement

Fig. 11 Computed primary consolidation settlement $S_{primary}$ at different depths by simplified Hypothesis B method

Fig. 12 Computed creep settlement S_{creep} at different depths by simplified Hypothesis B method

Fig. 13 Computed $S_{primary}$, S_{creepf} and S_{creepd} at the surface by simplified Hypothesis B method

Fig. 14 Comparisons of total settlement by simplified Hypothesis B method with different α, FE simulation and measurement

Fig. 15 Calculation results of total settlements with different creep parameters: (a) Case I; (b) Case II; (c) Case III

Fig. 16 Calculation results of total settlements with different permeability: (a) Case IV; (b) Case V

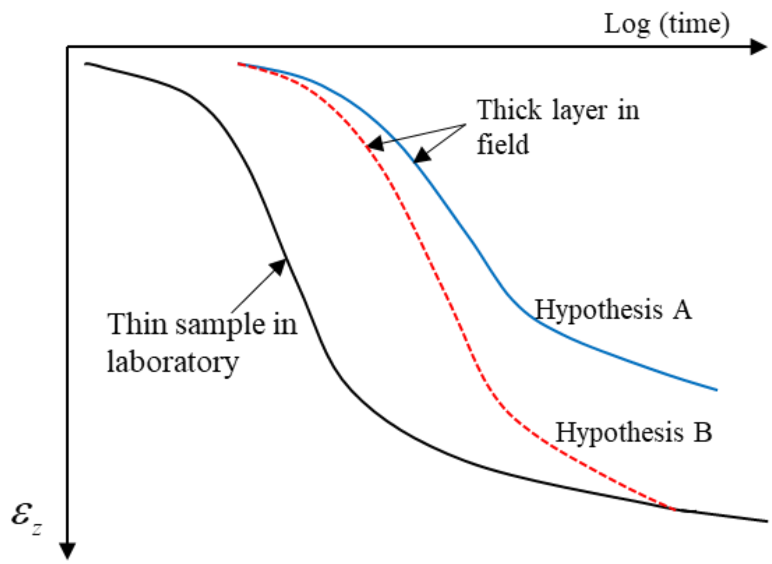

624

625 **Fig. 1** The schematic diagram of the difference between Hypothesis A and Hypothesis B

626

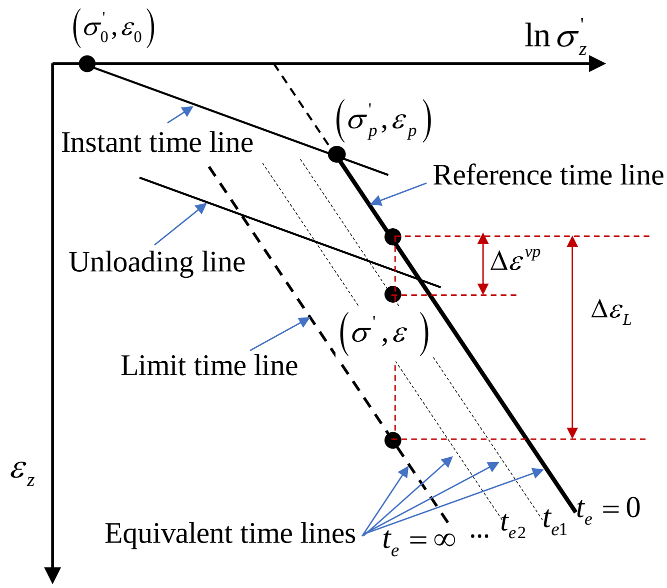

Fig.2 The schematic diagram of the 1-D nonlinear EVP model

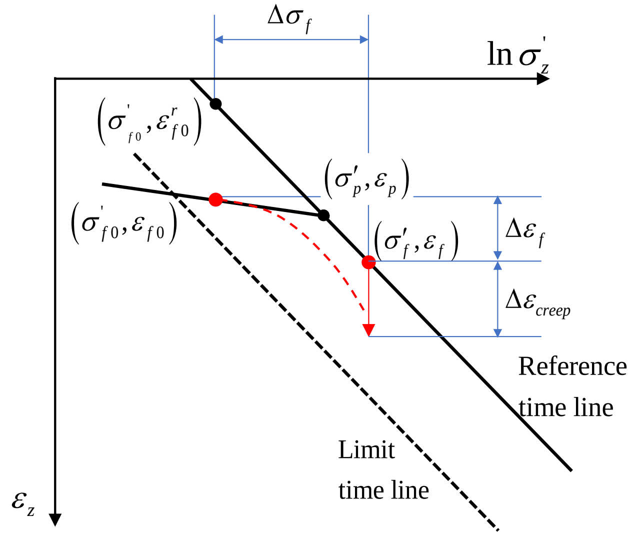

(a)

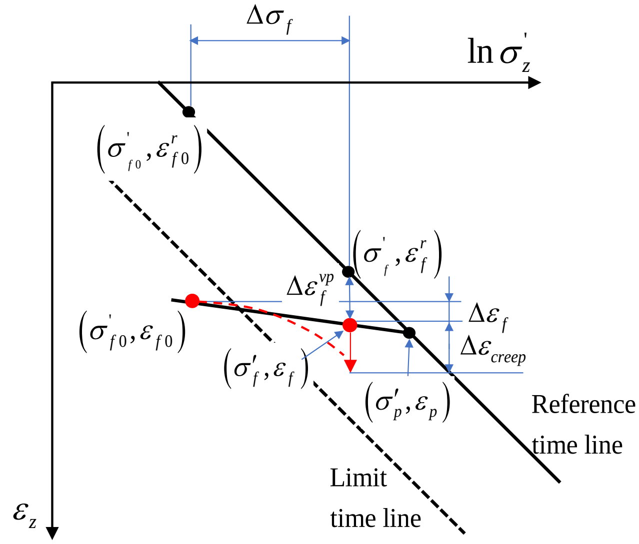

(b)

Fig.3 The schematic diagram of creep calculation when the final stress-strain of soil $(\sigma_f', \varepsilon_f)$ is at: (a) normally consolidation state and (b) over-consolidation state

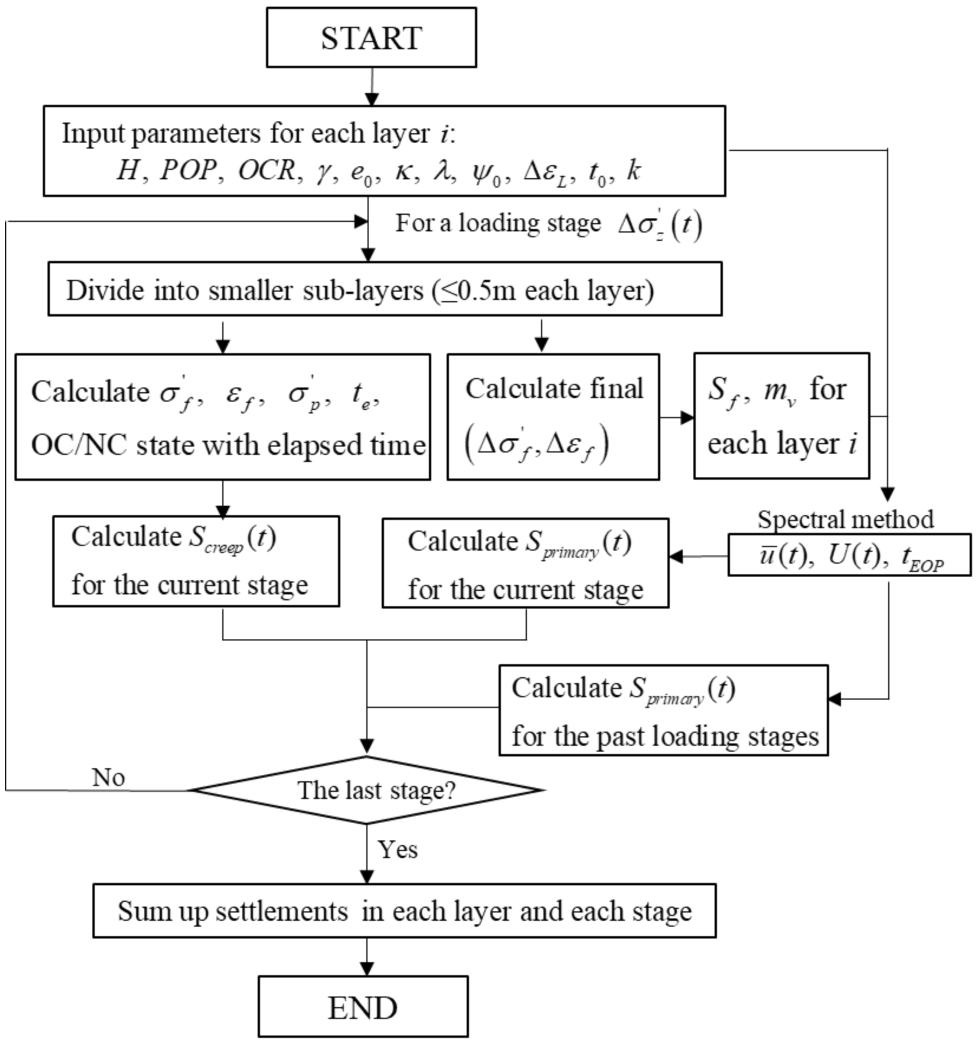

Fig.4 The calculation flow chart of the new simplified Hypothesis B method

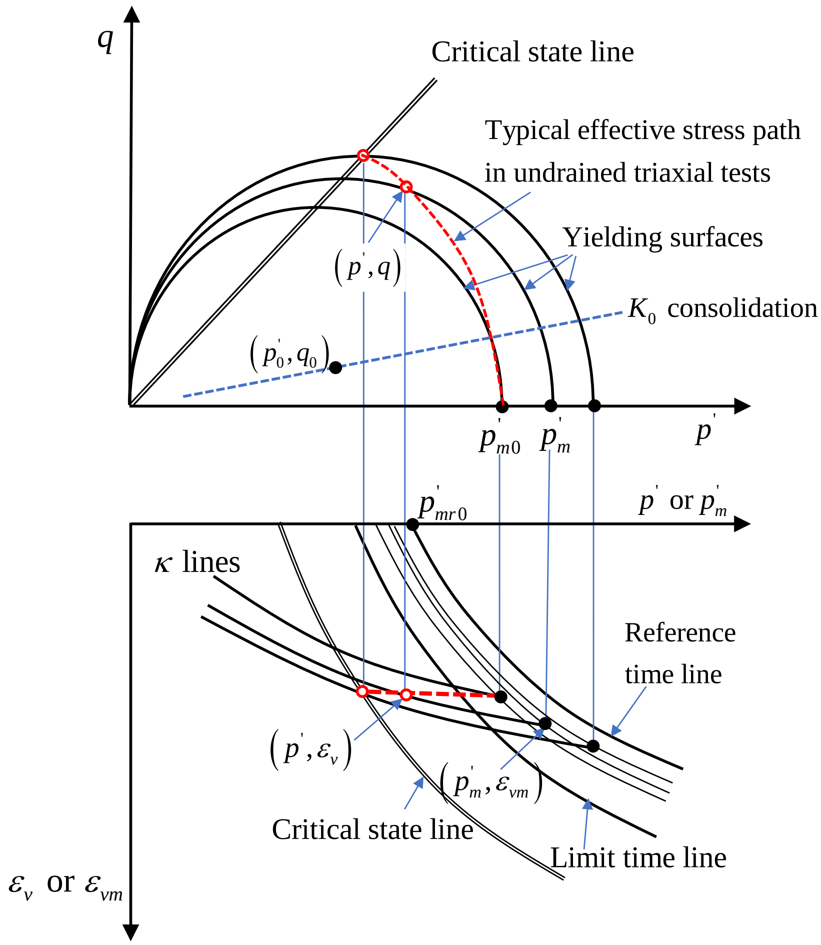

Fig.5 The schematic diagram of the 3-D nonlinear EVP model

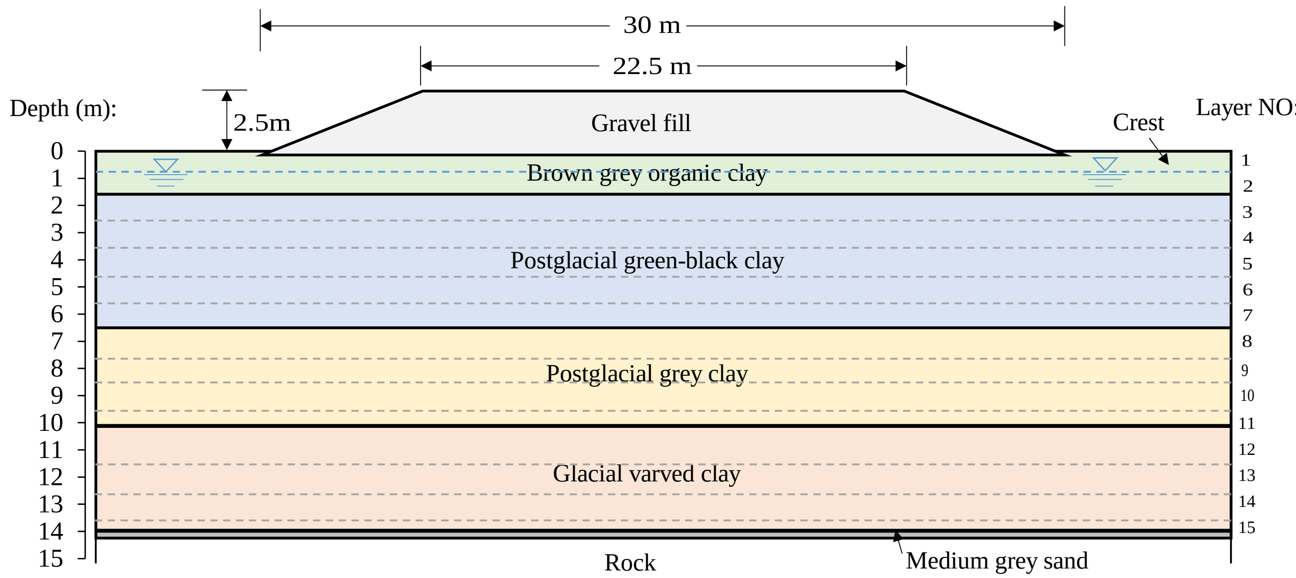

Fig.6 The ground profile of the Väsby embankment

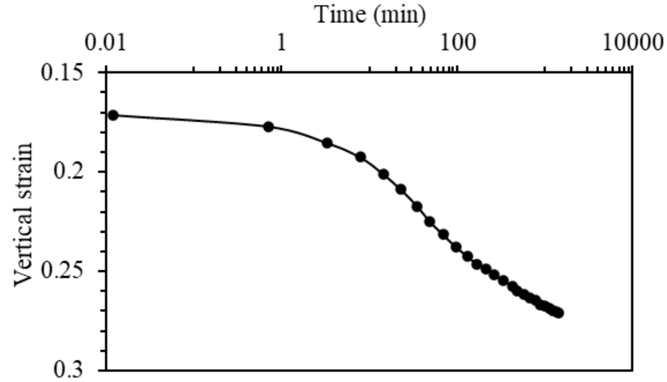
Time (min)
0.01
1
100
10000
0.15
0.2
0.25
0.3
Vertical strain

(a)

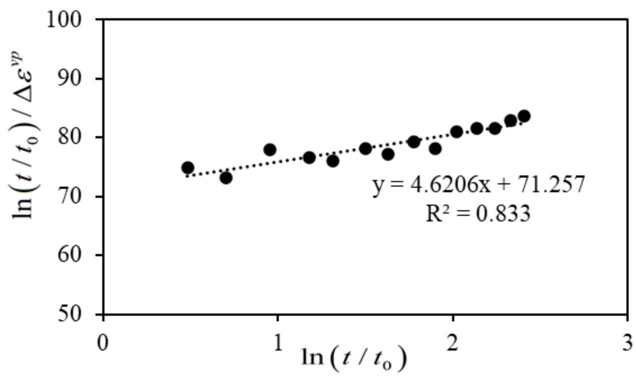
100
90
80
70
60
50
0
1
2
3
$\ln(t/t_0)/\Delta\varepsilon^{vp}$
$\ln(t/t_0)$
y = 4.6206x + 71.257
R² = 0.833

(b)

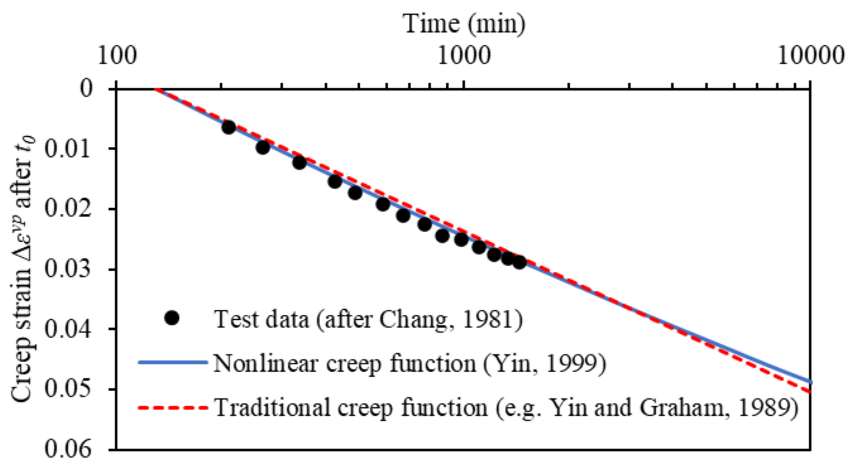
Time (min)
100
1000
10000
0
0.01
0.02
0.03
0.04
0.05
0.06
Creep strain $\Delta\varepsilon^{vp}$ after t_0
Test data (after Chang, 1981)
Nonlinear creep function (Yin, 1999)
Traditional creep function (e.g. Yin and Graham, 1989)

(c)

Fig.7 Fitting of creep parameters with the oedometer test results: (a) the original strain-log(time) curve; (b) plotting of $\ln\left(\frac{t_0+t}{t_0}\right)/\Delta\varepsilon^{vp}$ *v.s.* $\ln\left(\frac{t_0+t}{t_0}\right)$; (c) comparison between fitting results and test data

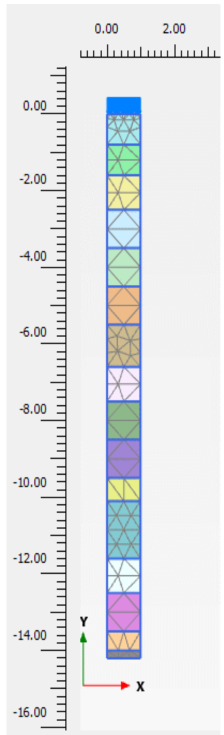

Fig. 8 Numerical model in Plaxis with mesh

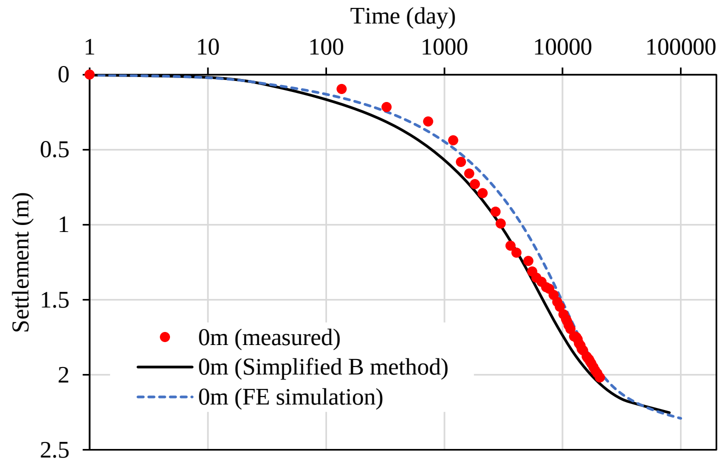
Time (day)
1
10
100
1000
10000
100000
0
0.5
1
1.5
2
2.5
Settlement (m)
0m (measured)
0m (Simplified B method)
0m (FE simulation)

(a)

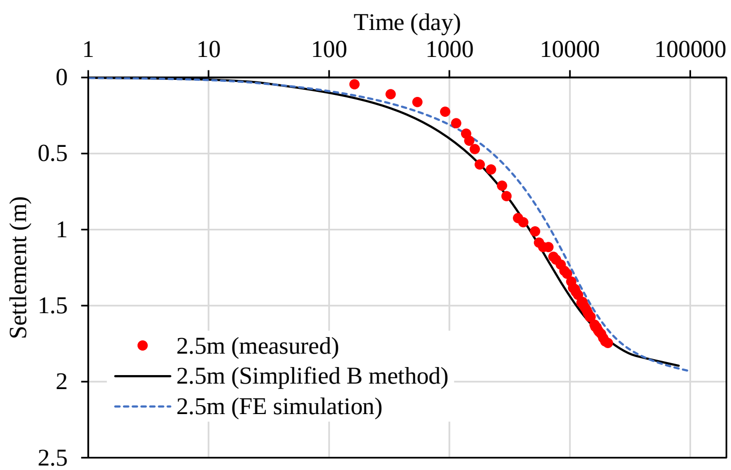
Time (day)
1
10
100
1000
10000
100000
0
0.5
1
1.5
2
2.5
Settlement (m)
2.5m (measured)
2.5m (Simplified B method)
2.5m (FE simulation)

(b)

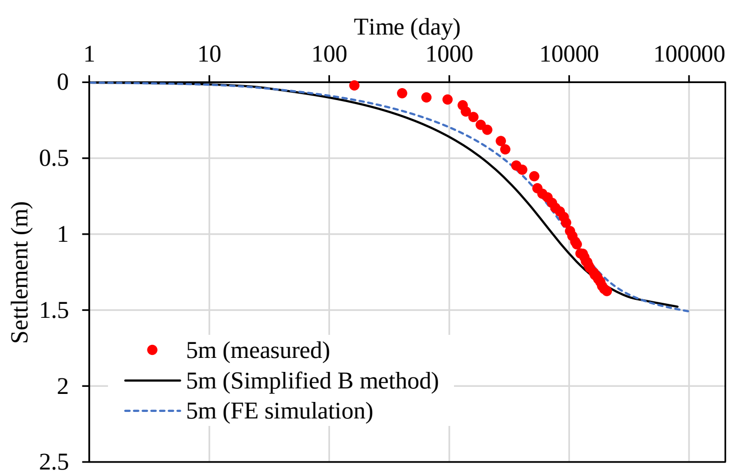
Time (day)
1
10
100
1000
10000
100000
0
0.5
1
1.5
2
2.5
Settlement (m)
5m (measured)
5m (Simplified B method)
5m (FE simulation)

(c)

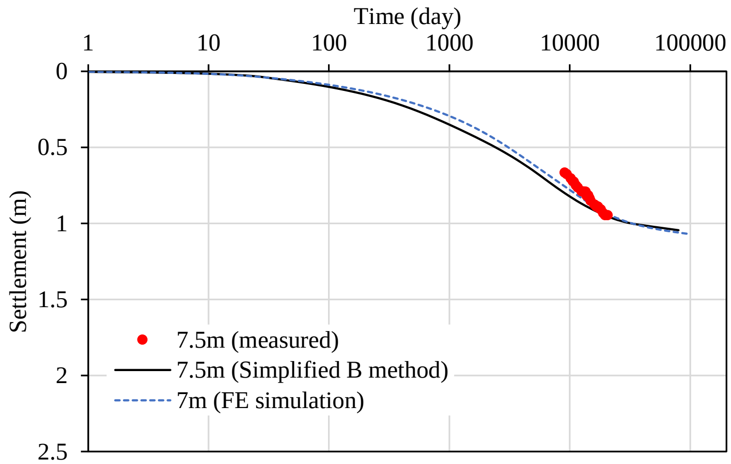

(d)

Fig. 9 Comparisons of settlement curves by simplified Hypothesis B method, FE simulations and measurement at different depths: (a) 0m; (b) 2.5m; (3) 5m and (4) 7.5m

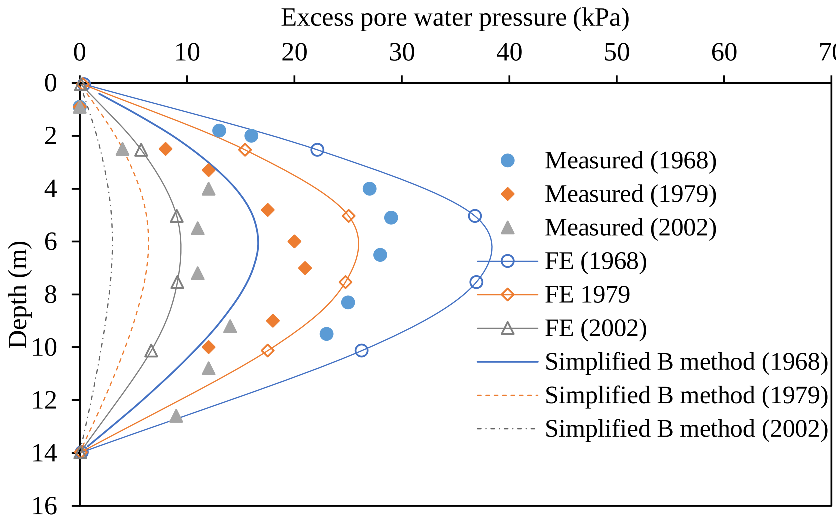

Fig. 10 Comparisons of excess pore pressure distributions in Years 1968, 1979 and 2002 by the new simplified method, FE simulation and in-situ measurement

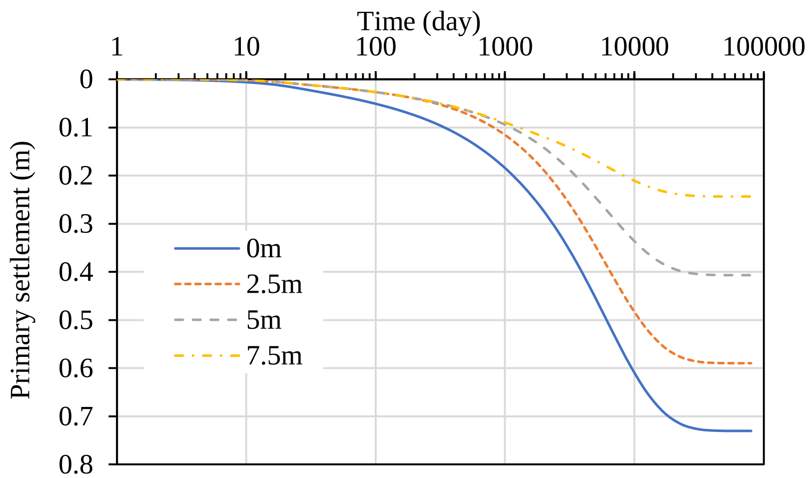

Fig. 11 Computed “primary” consolidation settlement $S_{primary}$ at different depths by the new simplified Hypothesis B method

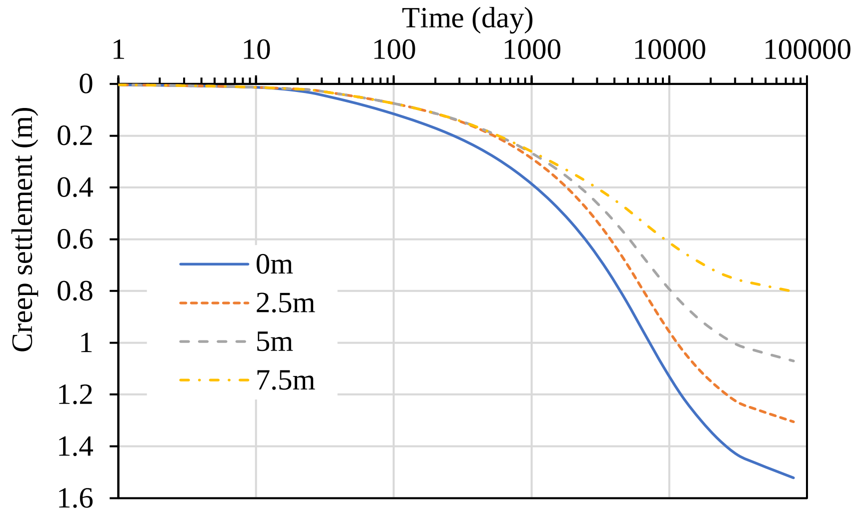

Fig. 12 Computed creep settlement S_{creep} at different depths by the new simplified Hypothesis B method

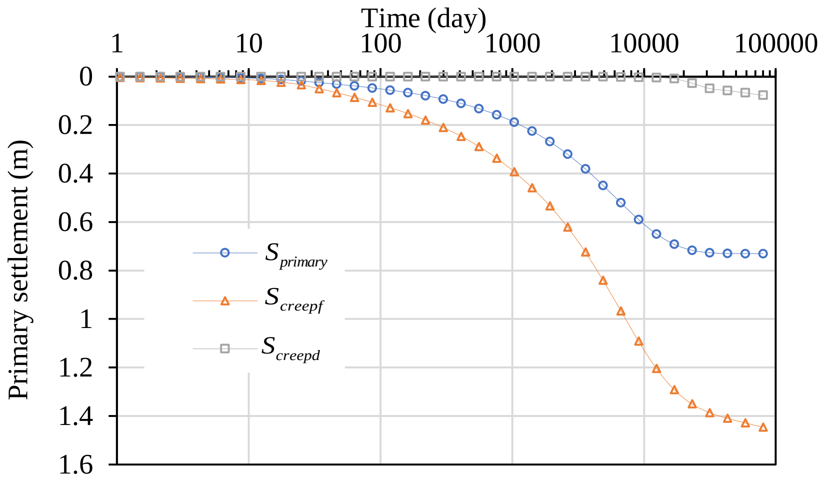

Fig. 13 Computed $S_{primary}$, S_{creepf} and S_{creepd} at the surface by the new simplified B method

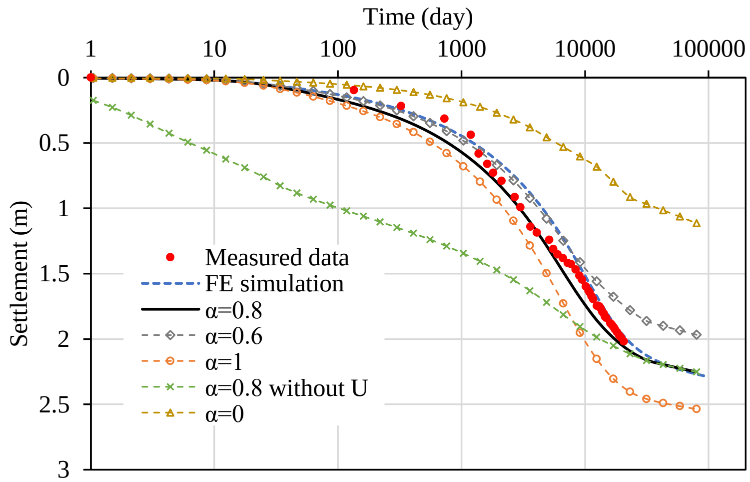

Fig. 14 Comparisons of total settlement by the new simplified B method with different α , FE simulation, and measurement

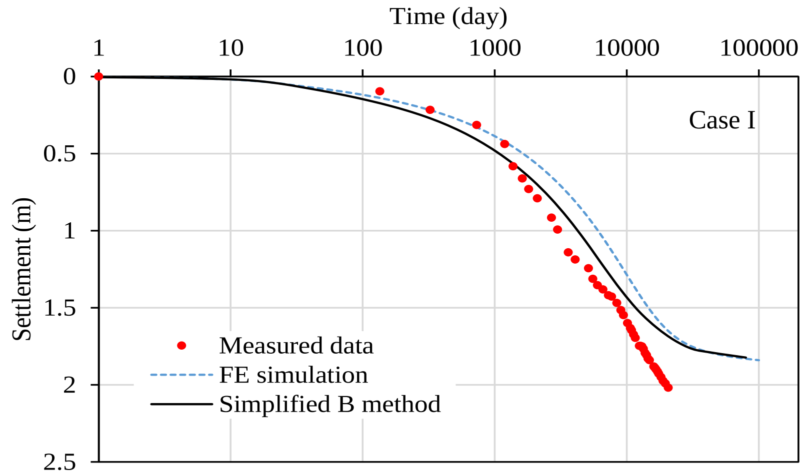
Time (day)
1
10
100
1000
10000
100000
0
0.5
1
1.5
2
2.5
Settlement (m)
Case I
Measured data
FE simulation
Simplified B method

(a)

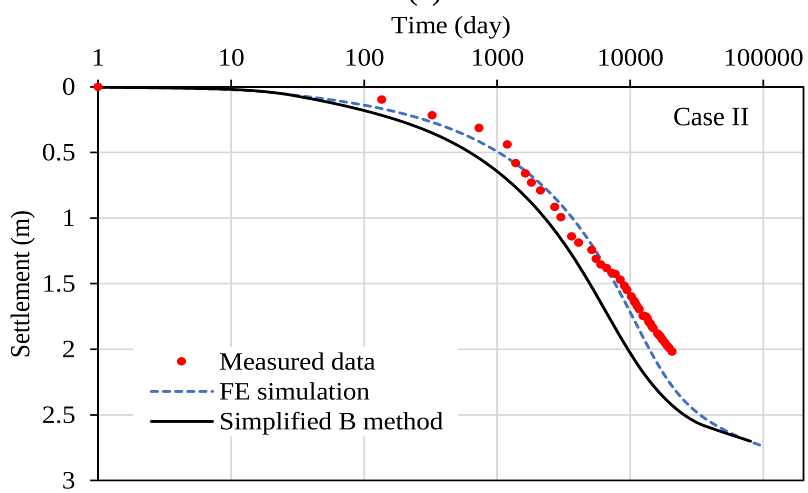
Time (day)
1
10
100
1000
10000
100000
0
0.5
1
1.5
2
2.5
3
Settlement (m)
Case II
Measured data
FE simulation
Simplified B method

(b)

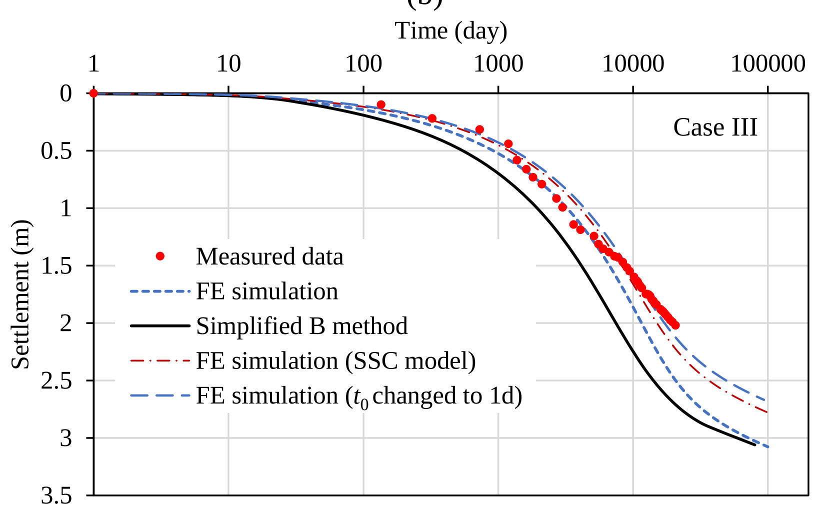
Time (day)
1
10
100
1000
10000
100000
0
0.5
1
1.5
2
2.5
3
3.5
Settlement (m)
Case III
Measured data
FE simulation
Simplified B method
FE simulation (SSC model)
FE simulation (t_0 changed to 1d)

(c)

Fig. 15 Calculation results of total settlements with different creep parameters: (a) Case I; (b) Case II; (c) Case III

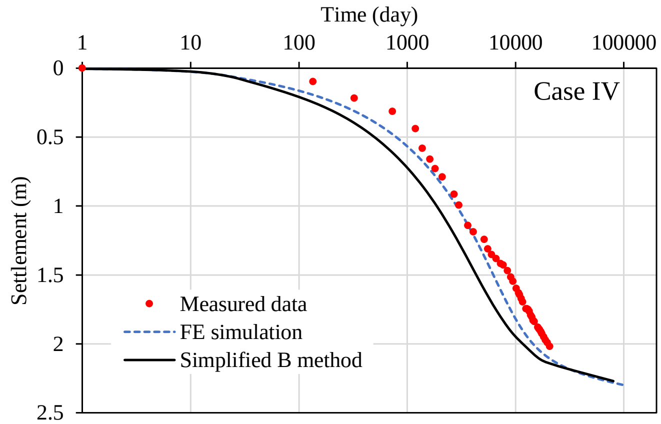

(a)

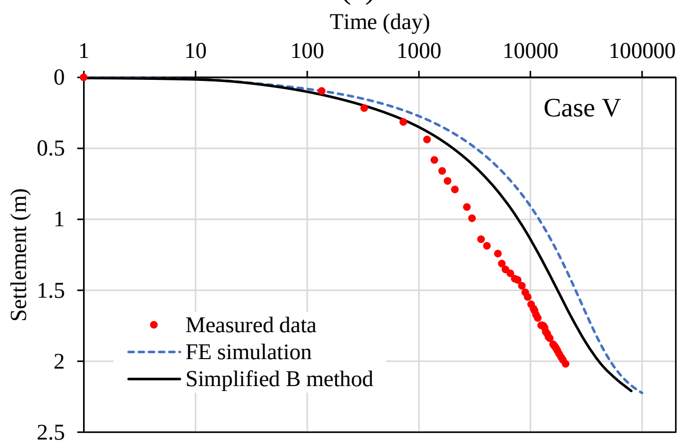

(b)

Fig. 16 Calculation results of total settlements with different permeability: (a) Case IV; (b) Case V

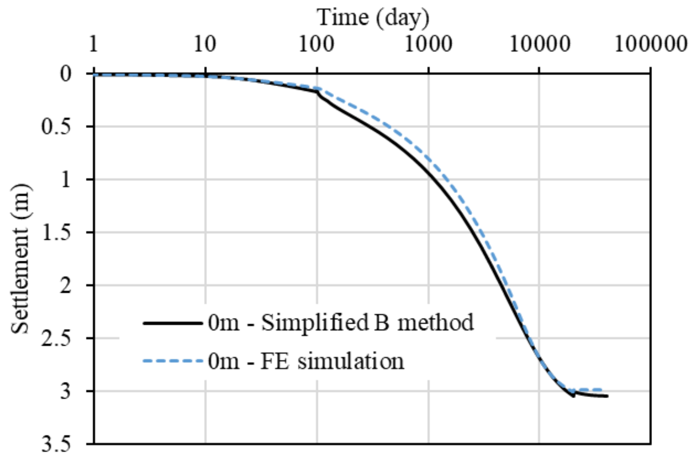
Time (day)
1
10
100
1000
10000
100000
0
0.5
1
1.5
2
2.5
3
3.5
Settlement (m)
0m - Simplified B method
0m - FE simulation

(a)

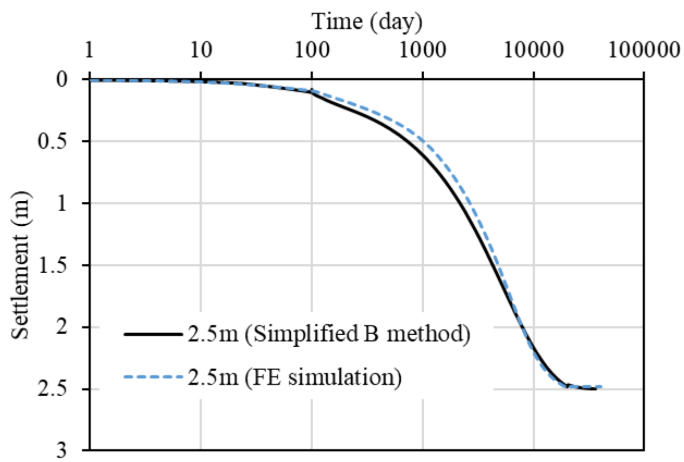
Time (day)
1
10
100
1000
10000
100000
0
0.5
1
1.5
2
2.5
3
Settlement (m)
2.5m (Simplified B method)
2.5m (FE simulation)

(b)

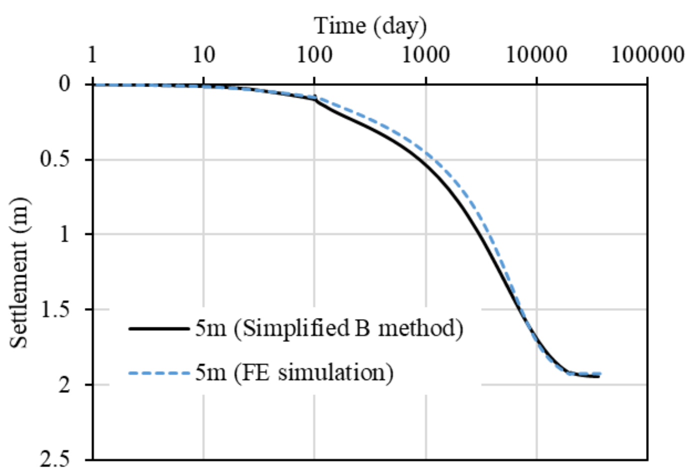
Time (day)
1
10
100
1000
10000
100000
0
0.5
1
1.5
2
2.5
Settlement (m)
5m (Simplified B method)
5m (FE simulation)

(c)

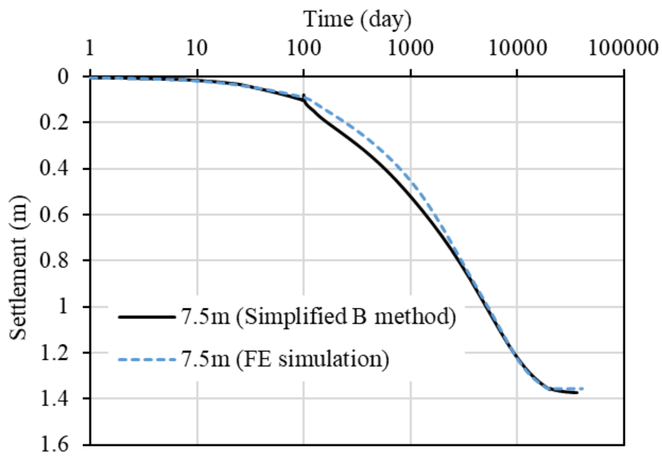

(d)

Fig. 17 Calculation results of total settlements under multi-staged loadings

List of tables

Table 1 Soil parameters for Väsby embankment

Soil type	Layer No.	H (m)	POP (kPa)	γ (kN/m^3)	κ	λ	ψ_0	$\Delta\varepsilon_L$	t_0 (min)	$1+e_0$	k_v (10^{-5} m/d)
Brown grey organic clay	1	0.8	44.9	13*	0.0548	0.369	0.058	0.23	130	3.9	4.23
	2	0.8	36.3	19	0.0548	0.369	0.058	0.23	130	3.9	4.23
Post glacial green black clay	3	0.9	4.3	13.3	0.047	0.536	0.058	0.21	130	4.26	4.67
	4	1	6.0	13.7	0.0317	0.401	0.058	0.23	130	3.9	4.54
	5	1	7.2	14.0	0.0343	0.494	0.058	0.24	130	3.79	4.45
	6	1	10.1	14.3	0.0109	0.505	0.058	0.26	130	3.48	4.58
	7	1.1	5.5	14.7	0.0109	0.505	0.058	0.26	130	3.48	4.54
Post glacial grey clay	8	0.9	10.8	15.0	0.0043	0.365	0.058	0.30	130	3.01	4.75
	9	1	16.0	15.3	0.0043	0.365	0.058	0.30	130	3.01	5.27
	10	1	10.6	15.7	0.0119	0.355	0.058	0.30	130	2.99	5.27
	11	0.6	16.0	16.0	0.0119	0.355	0.058	0.30	130	2.99	5.36
Glacial varved clay	12	1.5	19.6	16.3	0.0151	0.592	0.058	0.28	130	3.17	5.27
	13	0.9	13.0	16.7	0.0079	0.460	0.058	0.31	130	2.88	5.23
	14	1	8.6	17.0	0.0007	0.328	0.058	0.35	130	2.6	5.18
	15	0.5	4.5	17.0	0.0005	0.261	0.058	0.38	130	2.38	5.18

(H is the thickness. γ is unit weight . γ with * is unit weight for unsaturated soils in the crust above ground water level. $POP = \sigma'_{zp} - \sigma'_{z0}$ is called pre-over-consolidation pressure in history. k_v is the vertical permeability.)

Table 2 Creep parameters for parametric study

	Case I	Case II	Case III	Original case
$\Delta\varepsilon_L$	0.1	$\frac{e}{1+e_0}=0.651$	$+\infty$ or 10000	0.22
ψ_0	0.0747	0.0512	0.0482	0.0582
Δe_L	0.415	2.7	$+\infty$ or 10000	0.898

Table 3 Values of permeability for parametric study

Case name Soil type	Layer No.	Case IV	Case V	Original case
		Initial k_v (10^{-5} m/d)	Final k_v (10^{-5} m/d)	Average k_v (10^{-5} m/d)
Brown grey organic clay	1	6.91	1.56	4.23
	2	6.91	1.56	4.23
Post glacial green black clay	3	7.78	1.56	4.67
	4	7.34	1.73	4.54
	5	6.91	1.99	4.45
	6	6.48	2.68	4.58
	7	5.62	3.46	4.54
Post glacial grey clay	8	6.74	2.76	4.75
	9	7.78	2.76	5.27
	10	8.21	2.33	5.27
	11	8.64	2.07	5.36
Glacial varved clay	12	8.64	1.90	5.27
	13	8.64	1.81	5.23
	14	8.64	1.73	5.18
	15	8.64	1.73	5.18